# Densification and Grain Growth during the Sintering of Nanoscale SiC

M. Bothara*, S.V. Atre*, S.J. Park**, R.M. German**, T.S. Sudarshan*** and R. Radhakrishnan***

*Oregon Nanoscience and Microtechnologies Institute,
106 Covell Hall, Oregon State University, OR 97330 sundar.atre@oregonstate.edu
**Center for Advanced Vehicular Systems,
Mississippi State University, MS 39372, USA, sjpark@cavs.msstate.edu
***Materials Modification Inc., Fairfax, VA, USA, sudarshan@matmod.com

## ABSTRACT

Densification of nanoscale silicon carbide (SiC) was achieved using a novel method called Plasma Pressure Compaction ($P^2C$). Extremely fast sintering at temperatures lower than those used conventionally for SiC resulted in grain sizes between 500-700 nm. The grains depicted the core-rim type structure. Hardness and indentation toughness values were similar to those obtained for SiC by conventional methods. Hardness value decreased with an increase in the grain size.

*Keywords*: nanoscale, silicon carbide, sintering, plasma pressure compaction, hardness.

## 1 INTRODUCTION

Silicon carbide (SiC) is a covalently bonded material that exhibits a unique combination of properties such as very high hardness, good thermal shock resistance, high wear resistance and chemical inertness at elevated temperatures. Kamigatio [1] has suggested that nanoscale microstructures can lead to improved strength in mechanical ceramics. Kim *et al* [2] have developed SiC based ceramics which have grain sizes on the order of a few hundred nanometers. They have shown that these ceramics could be superplastically deformed at 1700 °C. Nano-SiC reinforced with $Si_3N_4$ exhibits enhanced strength and toughness properties on annealing [3,4].

The most common method of fabricating bulk SiC parts is by sintering. Sintering is a thermal treatment for bonding particles into a coherent, predominantly solid structure via mass transport events that often occur on the atomic scale [5]. The mass transport can occur either by solid state diffusion of atoms or by motion of atoms through a liquid phase. The self-diffusion of SiC is extremely small [6] and hence, various additives are used to assist sintering. The pioneering work of Prochazka [7], to use B and C as solid state sintering aids for SiC, was followed by the discovery of liquid phase sintering using oxide additives like $Al_2O_3$ and $Y_2O_3$ [8] and oxynitrides like AlN and $Y_2O_3$ [9,10]. The additives, along with the $SiO_2$ on the surface of the powder particles, melt at a lower temperature. The liquid phase formed as a result of the melting of the additives, facilitates mass transport that enhances densification.

Conventionally SiC is densified by hot pressing or pressureless sintering [7,8]. Recently, new methods have been developed such as plasma pressure compaction ($P^2C$) [11] that generate significantly higher densification rates thereby preventing excessive grain growth. The aim of the proposed research was to investigate the densification of nanoscale SiC in a $P^2C$ system and study the effect of the sintering time and temperature on the grain growth behavior and on the mechanical properties such as hardness and toughness.

## 2 PLASMA PRESSURE COMPACTION

Material Modification Inc., Fairfax, VA has developed a novel sintering technique called the Plasma Pressure Compaction ($P^2C$). The powder to be compacted is filled in a graphite die and placed between two electrodes as shown in Figure 1. The whole assembly is inside a vacuum chamber. When pulsed electrical power is applied, the current does not flow freely through the powder compact since an effective current path has not, as yet, been established due to the voids inside the powder. The oxide layer on the surface of the powder particle acts as an insulator at the particle contact. This causes a charge buildup at the interparticle gaps between the powder particles, which causes one particle to be charged negatively with respect to the other particles that are in contact with it. As the charge builds up, the voltage difference becomes sufficiently large to generate sparks that trigger an ionization process. It has been hypothesized that an inter-particle plasma activates the surface of the powder particles by removing the oxide and other contaminants.

Subsequently the powder compact is heated to release any adsorbed gas and/or moisture. This is usually indicated by drop in the initial vacuum level ($\sim 10^{-3}$ Torr). At this stage, an external uniaxial pressure of approximately 20-30 MPa is applied so as to facilitate sufficient current path through the powder compact. Application of the pulse current ends once the vacuum has reached its initial value. In the following stage, a constant current is applied so as to achieve the sintering temperature. Direct application of the current and the external uniaxial pressure serve to accelerate densification of the material by inducing

resistance heating and causing plastic deformation at the interparticle contact surfaces. The resistance heat serves to concentrate the heat at interparticle points of contact and the concurrent application of light pressure results in densification of the compact. The amount of pressure applied and the direct current required to reach the sintering temperature are determined by various factors such as the conductivity of the powder, particle size and also the dimensions of the graphite dies used. A schematic of the $P^2C$ equipment is shown in Figure 1.
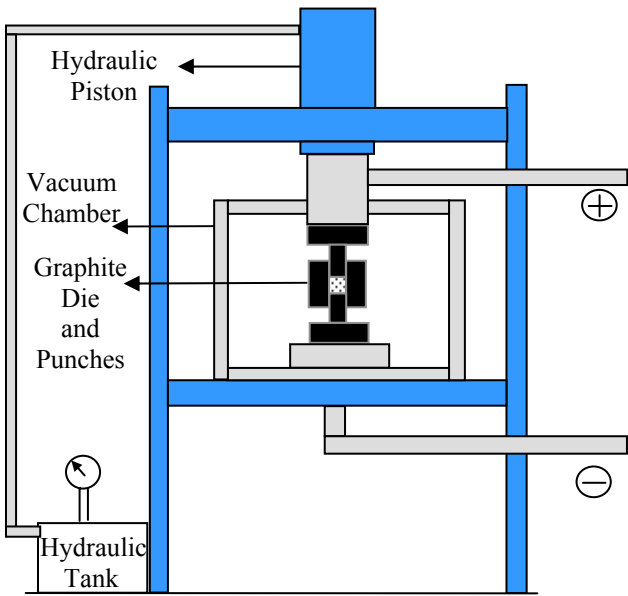


Figure 1: Schematic of the Plasma Pressure Compaction System at Materials Modification Inc., VA.

## 3 EXPERIMENTAL METHODS

### 3.1 Processing of Nanoscale SiC

α-SiC powder was mixed with AlN and $Y_2O_3$ as sintering aids in a rotary mill for 24 hrs using $ZrO_2$ pellets as the milling media. The milled powder mixture was consolidated using the $P^2C$ system. Six samples of 50 mm diameter were fabricated in this manner under different time-temperature combinations. The density for all the samples were measured by the Archimedes' method and found to be >99.5% of the theoretical value. Table 1 lists the experimental conditions for all the samples.

|          | 300 s    | 900 s    | 1800 s   |
|----------|----------|----------|----------|
| 1700 °C  | Sample 1 | Sample 2 | Sample 3 |
| 1850 °C  | Sample 4 | Sample 5 | Sample 6 |

Table1: Time-temperature combinations for six different samples prepared in $P^2C$.

## 3.2 Characterization

The sintered specimens were diamond ground to ~50 μm surface finish and then were polished to 1 μm finish using a diamond paste. The polished surfaces were etched in $CF_4$-10% $O_2$ plasma for 20 minutes. The grain morphology was observed using the scanning electron microscopy (SEM). Image-Pro Plus image analysis software was used to measure grain size from the SEM images of the samples in agreement with the ASTM E112.

Vickers hardness of the samples listed in Table 1 was measured in accordance with ASTM E384 using Leco microhardness tester. Vickers indenter with 1 kg load was used to measure the indentation fracture toughness of the nanoscale SiC samples in accordance with the method described by Anstis et al [12].

## 4 RESULTS AND DISCUSSION

### 4.1 Microstructure

SEM images of etched surfaces for the six samples listed in Table 1 are shown in Figure. 2.
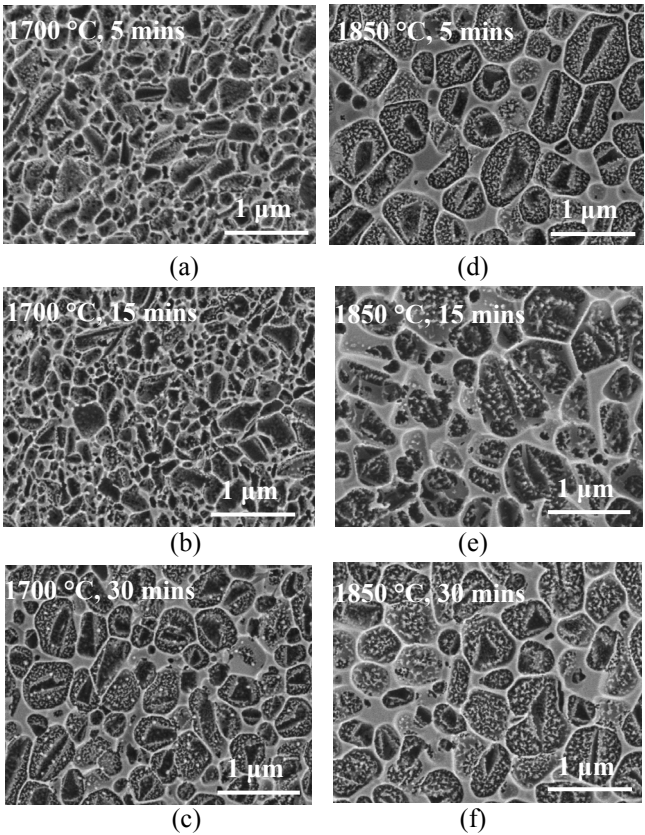


Figure 2: SEM micrographs for the six samples of Table 1.

The microstructures shown in Figure 2 are typical of SiC sintered with additives forming a liquid phase. In the present study, AlN and $Y_2O_3$ formed a liquid phase that promoted the mass transfer and thereby assisting the

sintering. The remnants of the liquid phase were present at the triple junctions. The core-rim structure that is seen in the micrographs in Figure 2 has been explained by Sigl *et al* [13] using the solution and reprecipitation mechanism. The small SiC grains dissolved in the liquid phase formed by the additives and then reprecipitated onto the large SiC grains. Thus the core (dark region) was rich in SiC and the rim (bright region) contained some amount of Al and Y. In Figures 2 (a) and (b), which correspond to samples sintered at 1700 °C for 5 minutes and 15 minutes respectively, the grains were mostly black indicating that minor amount of diffusion of Al and Y in the SiC grains occurred. As the sintering time or the temperature increased (Samples 3-6), the amount of the core region in the grains decreased progressively, thus indicating considerable amount of Al and Y diffusion.

## 4.2 Grain Size Measurements

As mentioned in Section 4.1, the amount of core region decreased with an increase in the sintering time or temperature. In order to quantify this effect, the fractional core area was measured for each sample. Fractional core area was defined as the ratio of the total core area to the total grain area in an image. Five images were analyzed for each sample. The plot in Figure 3 shows the results for the fractional core area and the grain size measurements of the nanoscale SiC samples.
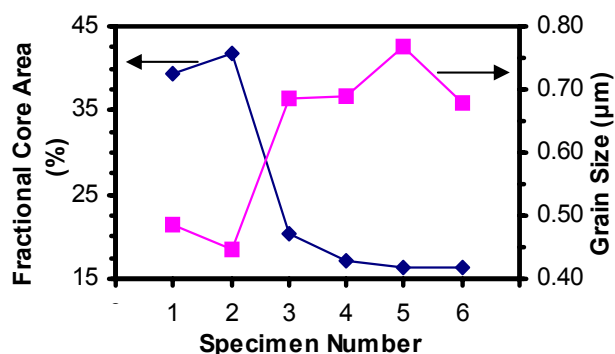
Figure 3: Fractional core area and grain size for the nanoscale SiC samples are plotted. The drop in the amount of core area coincides with the rise in the grain size.

The average grain size in Samples 1 and 2 was ~500 nm and the fractional core area was ~40%. In contrast the average grain size in Samples 3-6 was ~700 nm and the fractional core area was ~15%. Thus, at 1700 °C the grain size increased from 500 nm to 700 nm for an increase in the holding time from 900 s (sample 2) to 1800 s (sample 3). This increase in the grain size coincided with the reduction of the core area from 42% to 20%. On the other hand, for all the samples sintered at 1850° C the average grain size was ~700 nm but the size of the SiC core decreased and that of the rim portion of the grain increased as the sintering time increased.

## 4.3 Hardness

The hardness values for the nanoscale SiC samples at various indentation loads are shown in Figure 4. These hardness values are comparable to the hardness values of around 22 GPa, obtained by Schwetz *et al* [14]. Schwetz *et al* prepared their samples by hot pressing $\alpha$-SiC powder at 1960 °C for 1 h in the presence of AlN-$Y_2O_3$ and had the grain size of around 1.5 $\mu$m.
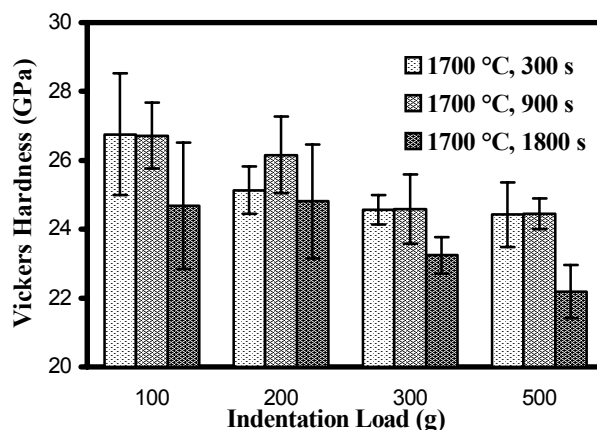
(a)
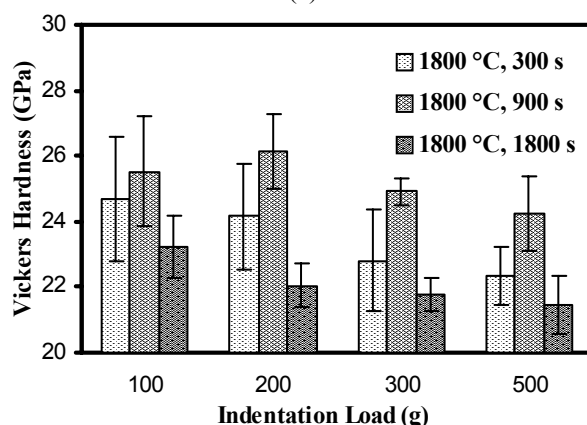
(b)

Figure 4: Vickers hardness as a function of load for the SiC samples sintered at three different times at (a) 1700 °C, (b) 1850 °C.

For the six nanoscale SiC samples, the hardness decreased with increasing load. This effect was more pronounced in the Samples 3-6 which had larger grain sizes as compared to the Samples 1 and 2. These trends suggested that at higher loads coarser-grained samples promoted room temperature grain boundary sliding more than the fine-grained materials [15]. The effect of grain size on the hardness of the nanoscale SiC samples is depicted in Figure 5. As grain size increased the hardness decreased. This trend is represented by the dotted line which is a linear fit to the experimental values of hardness for the nanoscale SiC samples.
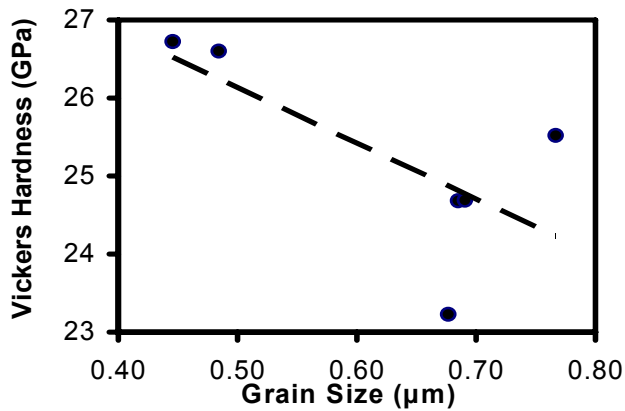
Figure 5: Effect of the grain size on the hardness of nanoscale SiC samples. The dotted line represents the linear fit to the measured hardness values.

## 4.4 Toughness

The indentation fracture toughness values obtained using a 1 kg load on a Vickers indenter are listed in Table 2 below. These toughness values are again similar to the values of around 3.5 $MPa.m^{1/2}$ that were obtained by Schwetz *et al* [14] for their SiC samples.

| Sample # | Temperature (°C) | Time (s) | Toughness ($MPa.m^{1/2}$) |
|---|---|---|---|
| 1 | 1700 | 300 | 4.8 ± 0.6 |
| 2 | 1700 | 900 | 3.4 ± 0.5 |
| 3 | 1700 | 1800 | 3.1 ± 0.3 |
| 4 | 1850 | 300 | 3.8 ± 0.7 |
| 5 | 1850 | 900 | 4.0 ± 0.5 |
| 6 | 1850 | 1800 | 3.8 ± 0.3 |

Table 2: Indentation fracture toughness for the six SiC samples.

The toughness values for all the samples ranged between 3 and 5 $MPa.m^{1/2}$. The scatter in the data suggests that this approach can only obtain an estimate of the actual fracture toughness. Further work is needed in performing standardized fracture toughness tests to better understand their microstructural origin.

## 5 CONCLUSIONS

Sintering of nanoscale SiC was achieved using a novel technique called the Plasma Pressure Compaction. Investigation was made into the effects of time and temperature on microstructure. It was observed that the grain size increased from 500 nm to 700 nm at 1700 °C with the increase in sintering time. The core-rim microstructure that is typical of SiC sintered with liquid phase forming additives was observed at higher temperatures or longer times. At 1850 °C the grain size

remained at around 700 nm with the development of the core-rim microstructure. The size of rim structure increased with the increase in sintering time and temperature. The resulting SiC samples had hardness values between 23 and 27 GPa and indentation toughness values between 3 and 5 $MPa.m^{1/2}$. It was also observed that the hardness value decreased with increasing grain size. These properties compare favorably with results obtained by hot pressing at increased cycle times and temperatures. These results suggest that even finer grain size may be possible with corresponding improvements in the properties.

## ACKNOWLEDGEMENT

## REFERENCES

1. O. Kamigaito, J. Jpn. Soc. Powder Metall., 38, 312-321, 1991.
2. Y.W. Kim, M. Mitomo and H. Hitrotsuru, J. Am. Ceram. Soc., 78, 3145-3138, 1995.
3. Y. I. Lee, Y. W. Kim, H. J. Choi and J. G. Lee, J. Kor. Ceram. Soc. 36, 799, 1999.
4. Y.W. Kim and M. Mitomo, J. Mat. Sci., 35, 5885-5890, 2000.
5. R.M. German, "Sintering Theory and Practice", John Wiley and Sons, Inc., NY, 1996.
6. J. Nadeau,, Bull. Am. Ceram. Soc., 52, 170-174, 1973.
7. S. Prochazka, Brit. Ceram. Res. Assoc., Special Ceramics 6, edited by P. Popper. 171-181, 1975.
8. M. Omori, and H. Takei, J. Am. Ceram. Soc., 65, C-92, 1982.
9. K. Y. Chia, W. D. G. Boecker, and R. S. Storm, U.S. Patent 5, 298, 470, 1994.
10. M. Nader, Doctoral thesis, University of Suttgart, 1995.
11. T.S. Srivatsan, B.G. Ravi, M. Petraroli and T.S. Sudarshan, Intl. J. Refrac. Metals and Hard Matls., 20, 181-186, 2002.
12. G.R.Anstis, P. Chantikul, B.R. Lawn and D.B. Marshall, J. Am. Ceram. Soc., 64, 533-538, 1981.
13. Sigi L. S. and Kleebe H. J., J. Am. Ceram. Soc., 76, 773-76, 1993.
14. Schwetz K.A., Kempf T., Saldsieder D. and Tel R., Ceram. Engr. and Sci. Proc., 25, 579-588, 2004.
15. Ray D., Flinders M., Anderson A. and Cutler R.M., Ceram. Engr. and Sci. Proc., 24, 401-410, 2003.